ACS OMEGA

http://pubs.acs.org/journal/acsodf

Article

New Functional Polymer Materials via Click Chemistry-Based Modification of Cellulose Acetate

Maximilian Röhrl, Justus F. Ködel, Renee L. Timmins, Christoph Callsen, Merve Aksit, Michael F. Fink, Sebastian Seibt, Andy Weidinger, Glauco Battagliarin, Holger Ruckdäschel, Rainer Schobert, Josef Breu,* and Bernhard Biersack*

Cite This: *ACS Omega* 2023, 8, 9889−9895

Read Online

ACCESS | Metrics & More | Article Recommendations | Supporting Information

ABSTRACT: Cellulose acetate (CA) was partially acrylated, and the resulting cellulose acetate acrylate (acryl-substitution degree of 0.2) underwent quantitative thio-Michael click reactions with various thiols. A toolbox of functional CA polymers was obtained in this way, and their properties were studied. The modification with fatty alkyl thiols led to hydrophobic materials with large water drop contact angles. Octadecylthio-, butoxycarbonylpropylthio-, and furanylthio-modifications formed highly transparent materials. The new derivative CAASFur disintegrated completely under industrial composting conditions. Films of modified CA polymers were cast and investigated in terms of barrier properties. The nanocomposite of CAAS18 compounded with a synthetic layered silicate (hectorite) of a large aspect ratio showed permeabilities as low as 0.09 g mm m^{-2} day^{-1} for water vapor and 0.16 cm^3 mm m^{-2} day^{-1} atm^{-1} for oxygen. This portfolio of functional CA polymers opens the door to new applications.

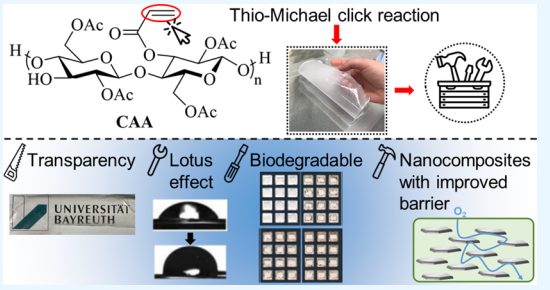

1. INTRODUCTION

Natural and re-growing sources for the preparation of functional polymer materials are getting more and more important.[1] Cellulose, for example, is an abundant polysaccharide accessible from plants. In particular, cellulose acetate (CA), obtained from acetylation of cellulose followed by partial deacetylation, can be applied for various purposes.[2] In addition, the degradation of CA by various mild methods was thoroughly studied.[3] Hence, CA can be an attractive surrogate for petrol-based polymers and plastics. However, CA also has disadvantages, such as insufficient water vapor barrier properties, which have prevented a wider application of this material so far.[4] Plasticizers are also needed to process cellulose acetate at low temperatures.[5] Modifications of CA such as cellulose acetate butyrate (CAB), cellulose acetate propionate (CAP), or cellulose acetate phthalate (CAPh) can overcome some of these drawbacks and improve the thermal and solubility properties as compared to unmodified CA.[6,7] Processing and mechanical properties of these materials are, however, still inadequate in comparison with other commodity polymers such as PP (polypropylene) and PE (polyethylene). Therefore, further efforts are needed in order to overcome these problems of CA-based polymers.[8]

The concept of "click chemistry" was initially described by Kolb, Finn, and Sharpless in 2001 and is a reasonable option for modifying polysaccharides in mild and quantitative ways.[9,10] The thiol-ene click reaction, for instance, has found numerous applications in material science.[11−13] Cellulose and cellulose derivatives such as CA were successfully modified via thiol-ene reactions.[14−16] These reports described complex reactions and modifications with expensive reagents and catalysts for synthesizing the precursors required for the thiol-ene reaction. A simple protocol for the acrylation of CA to generate the known acryl ester CAA (substitution degree of 0.2) was previously published.[17] In the present work, we describe the modification of CAA by the thiol-Michael reaction with various commercially available thiols, leading to new functionalized cellulose esters. Furthermore, by incorporating impermeable silicate nanosheets of delaminated hectorite (Hec) into a modified CAA, we were able to cast nanocomposite films that show excellent barrier properties.

2. MATERIALS AND METHODS

2.1. General. Cellulose acetate (medium M_n ∼ 30.000, 39.3−40.3 wt % acetyl) was obtained from Sigma Aldrich, and the other starting materials were purchased from Alfa Aesar (acryloyl chloride, 1-eicosanethiol, 1-hexadecanethiol), Fluka (1-octadecanethiol), Sigma Aldrich (butyl 3-mercaptopropionate, 1-dodecanethiol), and TCI (ethyl thioglycolate). CAA

Received: October 22, 2022
Accepted: January 17, 2023
Published: March 9, 2023

https://doi.org/10.1021/acsomega.2c06811
ACS Omega 2023, 8, 9889−9895

was prepared according to a literature procedure.[17] Infrared (IR) spectra: Perkin-Elmer Spectrum One FT-IR spectrophotometer with an ATR-sampling unit. Nuclear magnetic resonance (NMR) spectra: Bruker Avance 300 spectrometer, chemical shifts are given in parts per million (δ) downfield from tetramethylsilane as the internal standard.

2.2. Thiol-Michael Click Reaction: Typical Procedure. CAA (1.14 g, 0.03 mmol, substitution degree of 0.2) was placed in a flask and dissolved in DMSO (10 mL) under stirring, whereupon triethylamine (3 equiv) was added. Then, the respective thiol (6 equiv) was added and the reaction mixture was stirred at room temperature for 24 h. The product was precipitated by the addition of water (200 mL). The formed solid was collected by suction and washed twice with water (25 mL), followed by washing with EtOH (2 × 25 mL). The crude product obtained was dissolved in THF (50 mL), precipitated by the addition of *n*-pentane (200 mL), and collected. The filter cake was washed twice with *n*-pentane (25 mL). Yield: 90%. The ^{1}H NMR data given below list only selected signals of the thiol residues for better clarity, while the IR data and ^{13}C NMR data enumerate all bands and peaks of the product polymers.

2.2.1. CAAS12. Colorless solid; IR (ATR) ν = 3502, 2924, 2856, 1740, 1639, 1433, 1367, 1216, 1161, 1126, 1034, 952, 901, 836, 692 cm^{-1}; ^{1}H NMR (300 MHz, $CDCl_3$, δ): 0.85 (t, J = 6.3 Hz; dodecyl-Me), 1.2−1.4 (dodecyl-CH_2), 1.5−1.7 (dodecyl-CH_2); ^{13}C NMR (75.5 MHz, $CDCl_3$, δ): 14.1, 20.4, 20.6, 20.8, 22.7, 26.7, 28.9, 29.3, 29.6, 31.9, 32.2, 34.6, 62.0, 71.8, 72.8, 100.5, 169.3, 169.7, 170.2.

2.2.2. CAAS16. Colorless solid; IR (ATR) ν = 3452, 2924, 2854, 1739, 1644, 1435, 1367, 1317, 1221, 1162, 1127, 1031, 953, 901, 839, 811, 698 cm^{-1}; ^{1}H NMR (300 MHz, $CDCl_3$, δ): 0.85 (t, J = 6.3 Hz; hexadecyl-Me), 1.2−1.4 (hexadecyl-CH_2), 1.5−1.7 (hexadecyl-CH_2); ^{13}C NMR (75.5 MHz, $CDCl_3$, δ): 14.1, 20.5, 20.8, 22.7, 26.8, 28.9, 29.3, 29.6, 29.7, 31.9, 32.2, 34.6, 62.0, 71.8, 72.8, 100.5, 169.2, 169.7, 170.2.

2.2.3. CAAS18. Colorless solid; IR (ATR) ν = 3471, 2924, 2855, 1740, 1435, 1367, 1216, 1161, 1125, 1033, 952, 901, 840, 808 cm^{-1}; ^{1}H NMR (300 MHz, $CDCl_3$, δ): 0.85 (t, J = 6.3 Hz; octadecyl-Me), 1.2−1.4 (octadecyl-CH_2), 1.5−1.7 (octadecyl-CH_2); ^{13}C NMR (75.5 MHz, $CDCl_3$, δ): 14.1, 20.5, 20.8, 22.7, 26.7, 28.9, 29.3, 29.6, 29.7, 31.9, 32.2, 34.6, 62.0, 71.8, 72.8, 100.5, 169.3, 169.7, 170.2.

2.2.4. CAAS20. Colorless solid; IR (ATR) ν = 3473, 2924, 2851, 1739, 1632, 1436, 1410, 1367, 1319, 1218, 1164, 1124, 1031, 953, 900, 836, 809, 698 cm^{-1}; ^{1}H NMR (300 MHz, $CDCl_3$, δ): 0.84 (t, J = 6.3 Hz; eicosyl-Me), 1.2−1.3 (eicosyl-CH_2), 1.5−1.6 (eicosyl-CH_2); ^{13}C NMR (75.5 MHz, $CDCl_3$, δ): 14.1, 20.4, 20.5, 20.7, 22.6, 26.6, 28.9, 29.3, 29.6, 31.9, 32.0, 62.0, 71.8, 72.8, 100.5, 169.2, 169.7, 170.2.

2.2.5. CAASFur. Colorless solid; IR (ATR) ν = 3488, 2932, 1738, 1643, 1542, 1523, 1505, 1435, 1367, 1217, 1155, 1122, 1033, 956, 935, 902, 840, 744 cm^{-1}; ^{1}H NMR (300 MHz, $CDCl_3$, δ): 6.1−6.3 (furan-H), 7.3−7.4 (furan-H); ^{13}C NMR (75.5 MHz, $CDCl_3$, δ): 20.6, 20.8, 26.6, 28.5, 34.4, 62.0, 71.8, 72.8, 100.6, 107.9, 110.6, 142.4, 169.3, 169.7, 170.2.

2.2.6. CAASE2MA. Colorless solid; IR (ATR) ν = 3473, 2953, 2876, 1739, 1432, 1367, 1224, 1157, 1125, 1034, 900, 843, 685 cm^{-1}; ^{1}H NMR (300 MHz, $CDCl_3$, δ): 0.91 (t, J = 7.1 Hz; ethyl-Me), 4.07 (t, J = 7.1 Hz; ethyl-CH_2O); ^{13}C NMR (75.5 MHz, $CDCl_3$, δ): 14.2, 20.5, 20.6, 20.8, 27.6, 33.8, 34.9, 41.5, 45.4, 61.5, 62.1, 71.8, 72.8, 100.5, 169.3, 169.7, 170.2, 171.1.

2.2.7. CAASB3MP. Colorless solid; IR (ATR) ν = 3476, 2964, 2878, 1738, 1432, 1367, 1217, 1163, 1131, 1034, 952, 901, 839, 675 cm^{-1}; ^{1}H NMR (300 MHz, $CDCl_3$, δ): 0.91 (t, J = 7.4 Hz; butyl-Me), 1.3−1.4 (CH_2), 1.5−1.7 (CH_2), 4.07 (t, J = 6.7 Hz; butyl-CH_2O); ^{13}C NMR (75.5 MHz, $CDCl_3$, δ): 13.7, 19.1, 20.5, 20.6, 20.8, 26.9, 27.2, 30.6, 34.5, 34.8, 62.1, 64.6, 71.8, 72.8, 100.5, 169.2, 169.7, 170.2, 171.9.

2.3. Thermal Stability and Decomposition Behavior. Thermal decomposition was monitored by combined TG-DSC using a Linseis STA PT 1600 thermobalance with DSC sensor head type S. All specimens were investigated in air atmosphere using linear heating rates between r.t. and 1000 °C.

2.4. Contact Angle. Samples of polymer plates were prepared by the dissolution of the indicated polymers (0.5 g) in acetone (7 mL) and subsequent casting of the solution into a glass Petri dish with a diameter of 40 mm. The solvent evaporated completely in the open air overnight, leaving polymer foils in the Petri dishes, which were cut into pieces of 4 cm^2 for contact angle investigations. A drop of 10 μL of water was added to each sample, and the contact angles were investigated after 1 min by drop contour analysis using a Krüss G10 machine. Results are described as means of the left and right angles of each sample drop.

2.5. Transparency. For the preparation of the polymer films, the polymers were ground in a ball mill at 250 rpm for 1 h. The powder obtained was pressed to plates of 0.5 mm thickness in a melting press. Transmission, haze, and clarity of the polymer films were investigated with a BYK-Gardner Haze-Gard Plus hazemeter using visible light according to ISO 13468 (total transmittance) and ISO/DIS 14782 (transmission haze).

2.6. Disintegration Test under Industrial Composting Conditions. The test set-up was executed according to ISO 20200 Plastics—Determination of the degree of disintegration of plastic materials under simulated composting conditions in a laboratory-scale test (2015).

Films (thickness of 100 μm) of the polymer sample CAASFur were mounted on slide frames (12 replicates) and were positioned horizontally in a mixture of 1.2 kg of 14-weeks-old compost (provided by OWS, Belgium) sieved to a particle size of <10 mm and 0.3 kg of fresh vegetables in plastic boxes with holes for aeration. The samples were incubated at 58 ± 2 °C in the dark. The compost was mixed at regular intervals, the moisture content was checked and adjusted when needed, and the test items were visually monitored and scanned for documentation.

2.7. Barrier Properties. Samples of polymer films were prepared by dissolution of the indicated polymers (0.5 g) in acetone (7 mL) and casting the solution into a glass Petri dish with a diameter of 40 mm. For the preparation of the nanocomposite film, refer to chapter 2.8.

2.7.1. Water Vapor Transmission Rates. Water vapor transmission rate (WVTR) values of the casted nanocomposite and polymer films were measured on a Mocon PERMATRAN-W Model 3/33 (Mocon Inc., USA). The measurements were conducted at 23 °C and 85% RH. Sufficient time for moisture conditioning was guaranteed.

2.7.2. Oxygen Transmission Rates. Oxygen transmission rate (OTR) values of the casted nanocomposite and polymer films were determined by employing a Mocon OX-TRAN 2/21 (Mocon Inc., USA) at 23 °C and 50% RH. The CAAS18/Hec film was carefully equilibrated at 50% RH. A mixture of 98 vol % nitrogen and 2 vol % hydrogen gas was used as the

https://doi.org/10.1021/acsomega.2c06811
ACS Omega 2023, 8, 9889−9895

carrier gas and pure oxygen gas as the permeant (>99.95%, Linde Sauerstoff 3.5). Sufficient time for moisture conditioning was guaranteed.

2.7.3. Thickness Determination. The thickness of the casted films was determined by employing a High Accuracy Digimatic Micrometer (Mitutoyo, Japan) with a measuring range of 0−25 mm and a resolution of 0.1 μm.

2.8. Hectorite Nanocomposites. *2.8.1. Materials and Sample Preparation.* Synthetic clay sodium fluorohectorite (Hec, $[Na_{0.5}]^{inter}[Mg_{2.5}Li_{0.5}]^{oct}[Si_4]^{tet}O_{10}F_2$) was synthesized and annealed according to a published literature procedure.[18,19] For modification, 18-crown-6 (18C6) with 99% purity was provided by abcr GmbH, and *N*-methyl formamide (NMF) was used as a dispersant with 99% purity provided by Alfa Aesar.

A 4 wt % solution of CAAS18 in NMF was prepared by mixing overnight in an overhead shaker positioned in an oven set to 60 °C. The 18C6/Hec suspension (3 wt % Hec) was prepared by adding 0.15 g of Hec and an amount of 18C6 corresponding to 300% of the cation exchange capacity of Hec (0.151 g) to NMF, followed by mixing in an overhead shaker for three days. The suspension used to prepare the self-standing barrier film (total solid content 3.9 wt %) was prepared by adding 8.7 g of the CAAS18 solution to 1.3 g of the Hec suspension, followed by mixing overnight in an overhead shaker. This suspension was then cast in a Teflon dish (diameter of ∼80 mm) and transferred to an oven at 50 °C to dry for two weeks. To ensure complete solvent removal at the end of two weeks, the dish was transferred to a vacuum oven at 50 °C and 10^{-3} bar for 24 h before peeling the CAAS18/Hec film out of the dish.

2.8.2. Characterization of Nanocomposite Films. 2.8.2.1. X-ray Diffraction. The XRD pattern of the nanocomposite film was recorded on a Bragg−Brentano-type diffractometer (Empyrean, Malvern Panalytical BV, The Netherlands) using Cu K-α radiation (λ = 1.5406 Å). The diffractometer was equipped with a PIXcel-1D detector. All patterns were analyzed using Malvern Panalyticals's HighScore Plus software.

2.8.2.2. Transmission Electron Microscopy. Cross-sections were prepared from the films by employing a Leica Ultramicrotome UC-7 equipped with a diamond cutter type Diatome Ultra 35° MF-3763 at room temperature. TEM images of these cross-sections were recorded by applying a JEOL-JEM-2200FS (JEOL GmbH, Germany) microscope.

3. RESULTS AND DISCUSSION

Initially, acryl-modified CA (CAA) with an acryl-substitution degree of 0.2 was prepared by esterification of CA with acryloyl chloride.[17] CAA was used as the starting material for the thiol-Michael reactions with various thiols. Thiols with long alkyl chains such as dodecanethiol, hexadecanethiol, octadecanethiol, eicosanethiol, and esters such as ethyl 2-mercaptoacetate and butyl 3-mercaptopropionate, and with arenes such as furan-2-ylmethylthiol were applied as modifying agents of CAA (Scheme 1). Fatty alkyl modified CA derivatives CAAS12, CAAS16, CAAS18, and CAAS20, the ethyl ester CAASE2MA and butyl ester CAASB3MP, and the furanyl-modified CAASFur were synthesized in this way in high yields (90%). DMSO was used as a solvent for the click reactions, but THF was also applied successfully as an alternative organic solvent, leading to comparable yields. The modified polymer products showed excellent solubility in organic solvents such as acetone.

Scheme 1. Reagents and Conditions: Thiol (6 equiv), Et_3N (3 equiv), DMSO or THF, r.t., 24 h

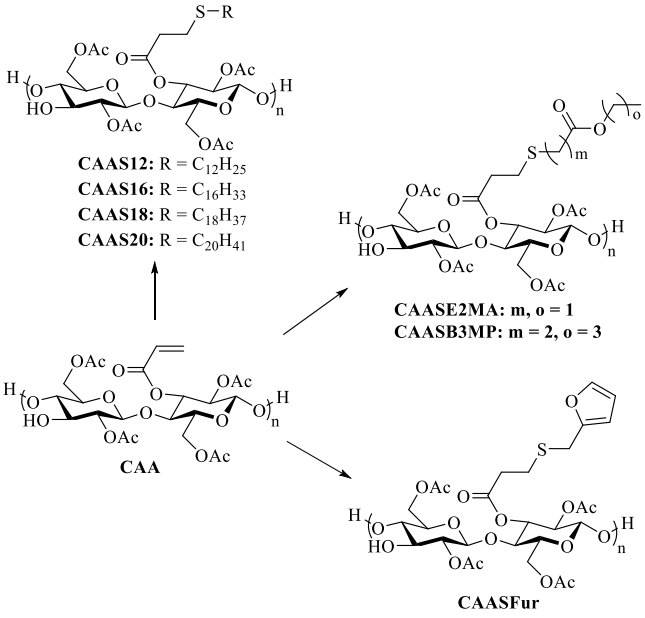

The obtained modified CA materials were colorless to off-white solids. They were analyzed by NMR and IR spectroscopy (see the Supporting Information for original ^{1}H and ^{13}C NMR spectra). The fatty alkyl rests of polymers CAAS12−20 are clearly visible in the NMR and IR spectra. Strong alkyl bands between 2800 and 3000 cm^{-1} were observed in the IR spectra. A weak broad signal between 3400 and 3500 cm^{-1} indicates the presence of hydroxyl groups, which were kept in the new polymer molecules at the carbohydrate backbone in line with the acryl-substitution degree of 0.2. ^{1}H NMR spectra displayed distinct peaks for the terminal methyl groups at δ = 0.84−0.85 ppm, as well as strong methylene signals at δ = 1.2−1.7 ppm. The terminal methyl groups were also visible in the ^{13}C NMR spectra at δ = 14.1 ppm. Similar signals were observed in the NMR spectra of the ester-modified polymers CAASE2MA and CAASB3MP (^{1}H NMR, δ = 0.91 ppm, ^{13}C NMR, δ = 13.7 and 14.2 ppm). In contrast, the furanyl derivative CAASFur exhibited characteristic downfield signals in its NMR spectra, which can be attributed to the furanyl ring (δ = 6.1−6.3, 7.3−7.4 ppm in the ^{1}H NMR spectrum; 100.6, 107.9, and 110.6 ppm in the ^{13}C NMR spectrum). In the ^{1}H NMR spectra, the integrals of the signals attributed to the modification were in line with the acryl-substitution degree of 0.2 of the CAA starting compound.

Thermogravimetric analyses (TGA) and differential scanning calorimetry (DSC) of the modified CA polymers did not reveal significant differences when compared with pure CA (see the Supporting Information). The new polymer derivatives were amorphous solids without visible crystalline components nor with distinct melting points of crystalline components as to the obtained DSC spectra. Plates and foils of selected polymer derivatives were cast from solutions in acetone upon evaporation of the solvent and compared with casted plates made of CA.

3.1. Contact Angles. The contact angles of water drops on the surface of plates prepared from the alkyl-modified CA derivatives CAAS12, CAAS16, CAAS18, and CAAS20 were determined in order to evaluate the hydrophobic surface

https://doi.org/10.1021/acsomega.2c06811
ACS Omega 2023, 8, 9889−9895

properties of these polymers, and the results were compared with the contact angles observed for plates of the starting material CA and the hydrophobic synthetic polymer PS (Figure 1A). The contact angle depended on the fatty alkyl

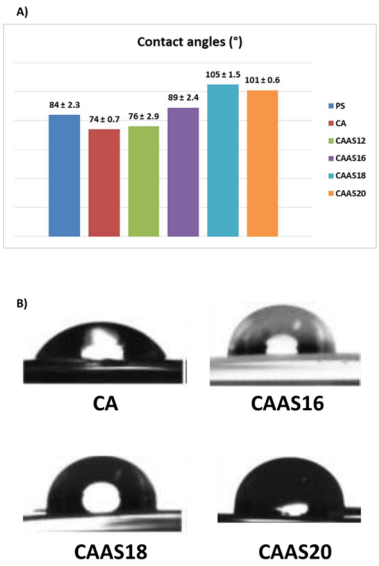

Figure 1. (A) Contact angles of water drops on plates made from derivatives CAAS12-20 or from the control polymers PS and CA after 1 min (means of the left and right angles). (B) Representative images of water drops on the indicated polymer plates after 1 min.

chain and as expected, increased with longer alkyl chains. Hence, polymers such as CAAS18 and CAAS20 had considerably more hydrophobic surfaces (contact angles above 100°) than CA (74°), PS (84°), and the close dodecyl and hexadecyl analogs CAAS12 (76°) and CAAS16 (89°) (Figure 1B).

3.2. Transparency. A hazemeter was used to determine the transparency parameters of the plates of the new polymer materials CAAS18, CAASB3MP, and CAASFur in comparison with plates of CA and PS. The plates of all three tested modified CA polymers exhibited improved optical properties in terms of transmission, haze, and clarity when compared with CA (Table 1). The modified polymers also showed trans-

Table 1. Transparency of CA Polymers CAAS18, CAASB3MP, and CAASFur in Comparison with PS and CA[a]

polymer	transmission (%)	haze (%)	clarity (%)
PS	94.2	4.72	95.8
CA	93.2	33.9	72.9
CAAS18	94.3	1.0	99.0
CAASB3MP	94.4	1.0	99.1
CAASFur	94.8	0.94	99.4

[a]Plates of 0.5 mm thickness were prepared from each sample for testing.

mission values similar to PS, as well as reduced haze and increased clarity compared to PS. These results indicate that the new polymers CAAS18, CAASB3MP, and CAASFur can be applied as transparent films/foils and plastic glass materials, which can replace oil-based plastics for these applications. The transparencies of these new CA-based polymers can be explained by a low or absent crystallinity and their strongly amorphous solid character, along with excellent solubility in low-boiling organic solvents. In nanocomposites of starch nanocrystals acetate (SNA) with hydrophobic cellulose laurate ester, the cellulose ester was the well-transmitting component whose transmission was reduced by increasing amounts of SNA.[20] The combination of high transparency with considerable hydrophobicity in cellulose acetate-based polymers can lead to valuable applications such as sensoring and electronics, UV protection, and packaging including active packaging.[21−25]

3.3. Disintegration under Industrial Composting Conditions. As a proof of principle, the polymer sample CAASFur was selected and its disintegration under industrial composting conditions was investigated according to ISO 20200. Films with a thickness of 100 μm were used for this experiment. Although disintegration does not give ultimate proof of complete biodegradation of the material, it can indicate the potential of the material to be biodegraded by natural microbes. The polymer sample passed the test successfully and disintegrated completely after 69 days (Figure 2). Substantial disintegration was already observed after 42 days.

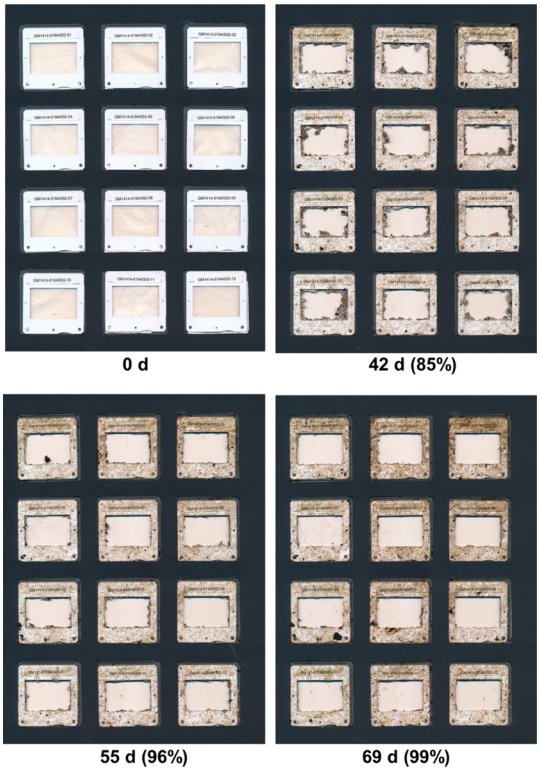

Figure 2. Time-dependent disintegration (in %) of the new polymer CAASFur under industrial composting conditions according to ISO 20200.

3.4. Barrier Properties and Nanocomposite Preparation. The water vapor barrier properties of some modified CA polymers were evaluated by measuring the water vapor transmission rates through casted films. With this sensitive measurement method, the hydrophobicity of the differently modified CA derivatives can be probed. However, gas transmission rates strongly depend on the thickness of the films, and therefore, the values were normalized to 1 mm, yielding water vapor permeability (WVP). Permeability values

https://doi.org/10.1021/acsomega.2c06811
ACS Omega 2023, 8, 9889−9895

Table 2. WVP and OP at 23 °C and Respective RH

polymer	WVP/g mm m^{-2} day^{-1} at 85% RH	OP/cm^3 mm m^{-2} day^{-1} atm^{-1} at 50% RH
CAAS16	36.4	
CAAS18	24.8	
CAAS20	9.9	
CAASB3MP	21.5	
CAAS18/Hec	0.09	0.16
PET	0.5−2	1−5
PP	0.2−0.4	50−100
PE	0.5−2	50−200
PS	1−4	100−150
PVC	1−2	2−8

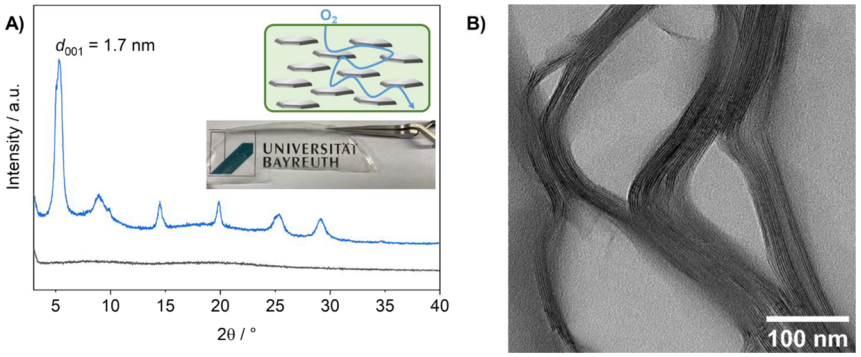

Figure 3. Characterization of the CAAS18/Hec nanocomposite film. (A) XRD pattern of the neat CAAS18 film (black) and CAAS18/Hec nanocomposite film (blue). Top inset sketches the tortuous path theory for an oxygen molecule. Bottom inset shows the transparent CAAS18/Hec nanocomposite film. (B) TEM image of the CAAS18/Hec cross-section indicating segregated domains of CAAS18 slabs (bright) and restacked Hec-only domains (dark).

facilitate comparison with other polymers (Table 2) at 85% relative humidity (RH).[26]

In general, the permeability (P) of a barrier material can be expressed as $P = S \times D$ with the solubility parameter (S) and diffusivity parameter (D) of the permeate.[27] Polar molecules like water are less soluble in hydrophobic matrices and vice versa. As expected, an increase in the chain length of the alkyl side groups of CAAS derivatives led to a decrease in the WVP due to a more hydrophobic character of the polymers (Table 2). Increasing the aliphatic chain length of the fatty alkyls from 16 carbons in CAAS16 to 20 carbons in CAAS20 reduced the WVP by more than a factor of three. This can be attributed to the reduced solubility parameter S. The butyl-ester-modified CAASB3MP ranks between the CAAS derivatives in terms of WVP. Nevertheless, the barrier values of neat polymer films were still distinctly below the requirements for food packaging and the specifications of commonly used polymer foils. Thus, further improvement is needed.

Compositing polymers with impermeable clay nanosheets improves the barrier properties of polymer matrices based on the tortuous path theory (Figure 3A top inset).[28] The incorporation of large aspect ratio synthetic sodium fluorohectorite (Hec) was shown to improve the WVP and oxygen permeability (OP) by orders of magnitudes.[29−32] To illustrate this concept for the new CA-based polymers presented in this study, CAAS18 was selected and mixed with a modified Hec, yielding a high barrier and transparent nanocomposite film upon drying (Figure 3A bottom inset).[33] The obtained CAAS18/Hec film showed WVP at 85% RH and OP at 50% RH as low as 0.09 g mm m^{-2} day^{-1} and 0.16 cm^3 mm m^{-2} day^{-1} atm^{-1}, respectively. Hereby, the WVP of the pristine CAAS18 could be reduced by 99.6% compared to the initial WVP of 24.8 g mm m^{-2} day^{-1}. Besides the hydrophobization arising from the fatty alkyl side groups in CAAS18, the modification of Hec additionally reduces its ability to swell in the presence of water vapor, explaining the solid WVP at a high 85% RH for the CAAS18/Hec nanocomposite.[33] While the suspensions applied for wet coating were homogeneous, segregation was observed upon drying. TEM images revealed separated domains of neat CAAS18 and restacked Hec-only domains with a thickness of up to 100 nm (Figure 3B). This thermodynamically induced phase segregation was further evidenced via XRD. The XRD pattern of CAAS18/Hec exhibits a basal spacing of 1.7 nm that can be assigned to the intercalated 18C6 crown ether complexing the sodium interlayer cation (Figure 3A).[27] Pure CAAS18 shows a typical XRD pattern of an amorphous polymer, which corroborates the observed transparencies and DSC spectra of CAAS18 and its closely related hydrophobic derivatives. The segregation might actually be advantageous when it comes to degradation. We could recently show that such phase segregation accelerates the biodegradation of nanocomposite films due to fragmentation and concomitantly increased the surface area by swelling of the Hec domains.[34] The transparent CAAS18/Hec nanocomposite film outperforms commonly applied packaging polymers like PET, PE, or PVC in terms of water vapor and oxygen barrier properties (Table 2), rendering these biobased materials promising alternatives for currently applied packaging materials.

4. CONCLUSIONS

In summary, we described a simple and efficient method for the preparation of a series of new CA-derived polymers with interesting and adjustable functionalities. For instance,

https://doi.org/10.1021/acsomega.2c06811
ACS Omega 2023, 8, 9889−9895

modified CA polymers with considerable barrier properties and hydrophobic surfaces were obtained this way. The barrier properties of CAAS18 were significantly improved by adding large aspect ratio nanosheets of a synthetic clay (hectorite), leading to nanocomposite materials with excellent water vapor and oxygen barriers. In addition, rapid disintegration of the cellulose polymers under laboratory industrial composting conditions was observed, proving the potential of these materials to be biodegraded by natural microbes. Hence, these modified CA derivatives could be an interesting alternative to conventional plastics, although further investigations based on respirometric methods are needed to prove their biodegradability. The described method also enables fine-tuning of materials by using appropriate thiol compounds for the thio-Michael click reaction.

■ ASSOCIATED CONTENT

Supporting Information

The Supporting Information is available free of charge at https://pubs.acs.org/doi/10.1021/acsomega.2c06811.

TGA/DSC spectra and NMR spectra of the new polymers (PDF)

■ AUTHOR INFORMATION

Corresponding Authors

Josef Breu − *Inorganic Chemistry 1, University of Bayreuth, 95440 Bayreuth, Germany;* orcid.org/0000-0002-2547-3950; Email: josef.breu@uni-bayreuth.de

Bernhard Biersack − *Organic Chemistry 1, University of Bayreuth, 95440 Bayreuth, Germany;* orcid.org/0000-0001-7305-346X; Email: bernhard.biersack@uni-bayreuth.de

Authors

Maximilian Röhrl − *Inorganic Chemistry 1, University of Bayreuth, 95440 Bayreuth, Germany*

Justus F. Ködel − *Fachgruppe Chemie, Wirtschaftswissenschaftliches und Naturwissenschaftlich-Technologisches Gymnasium Bayreuth, 95448 Bayreuth, Germany*

Renee L. Timmins − *Inorganic Chemistry 1, University of Bayreuth, 95440 Bayreuth, Germany*

Christoph Callsen − *Department of Polymer Engineering, Faculty of Engineering Science, University of Bayreuth, 95440 Bayreuth, Germany*

Merve Aksit − *Department of Polymer Engineering, Faculty of Engineering Science, University of Bayreuth, 95440 Bayreuth, Germany*

Michael F. Fink − *Chair of Electrochemical Process Engineering, Faculty of Engineering Science, University of Bayreuth, 95447 Bayreuth, Germany;* orcid.org/0000-0002-2039-4735

Sebastian Seibt − *Linseis Messgeräte GmbH, 95100 Selb, Germany*

Andy Weidinger − *Fachgruppe Chemie, Wirtschaftswissenschaftliches und Naturwissenschaftlich-Technologisches Gymnasium Bayreuth, 95448 Bayreuth, Germany*

Glauco Battagliarin − *Biopolymers and Biodegradability Research, BASF, 67056 Ludwigshafen am Rhein, Germany*

Holger Ruckdäschel − *Department of Polymer Engineering, Faculty of Engineering Science, University of Bayreuth, 95440 Bayreuth, Germany;* orcid.org/0000-0001-5985-2628

Rainer Schobert − *Organic Chemistry 1, University of Bayreuth, 95440 Bayreuth, Germany;* orcid.org/0000-0002-8413-4342

Complete contact information is available at: https://pubs.acs.org/10.1021/acsomega.2c06811

Author Contributions

The manuscript was written through the contributions of all authors. All authors have given approval to the final version of the manuscript. M.R. and J.F.K. contributed equally.

Notes

The authors declare no competing financial interest.

■ ACKNOWLEDGMENTS

J.K. was supported by the Stiftung Jugend forscht. J.B., H.R., and R.S. are grateful to the Deutsche Forschungsgemeinschaft (SFB 840 and SFB 1357− project number 391977956 −C02). The authors thank Dr. Robert Loos (Biopolymers and Biodegradability Research, BASF) for scientific advice and Marco Schwarzmann for preparing and taking the transmission electron microscopy images. We appreciate the support of the Keylabs for Polymer Additives and Fillers, Optical and Electron Microscopy, Mesoscale Characterization: Scattering Techniques, and Surface and Interface Characterization of the Bavarian Polymer Institute (BPI).

■ ABBREVIATIONS

CA, cellulose acetate; CAA, cellulose acetate acrylate; DMSO, dimethyl sulfoxide; DSC, differential scanning calorimetry; Hec, hectorite; NMF, *N*-methyl formamide; OP, oxygen permeability; PE, polyethylene; PET, polyethylene terephthalate; PP, polypropylene; PS, polystyrene; PVC, polyvinylchloride; RH, relative humidity; SNA, starch nanocrystals acetate; TEM, transmission electron microscopy; TGA, thermogravimetric analysis; THF, tetrahydrofuran; WVP, water vapor permeability; XRD, X-ray diffraction

■ REFERENCES

(1) Chen, G.-Q.; Patel, M. K. Plastics derived from biological sources: present and future: a technical and environmental review. *Chem. Rev.* **2012**, *112*, 2082−2099.

(2) Edgar, K. *Encyclopaedia of Polymer Science and Technology, Vol. 9. Organic cellulose esters*; Mark, H. F., Ed.; Wiley: New York, USA, 2004; pp. 129−158.

(3) Puls, J.; Wilson, S.; Hölter, D. Degradation of cellulose actetate-based materials: a review. *J. Polym. Environ.* **2011**, *19*, 152−165.

(4) Mostafa, N. A.; Farag, A. A.; Abo-dief, H. M.; Tayeb, A. M. Production of biodegradable plastic from agricultural wastes. *Arab. J. Chem.* **2018**, *11*, 546−553.

(5) Phuong, V. T.; Verstiche, S.; Cinelli, P.; Anguillesi, I.; Coltelli, M.-B.; Lazzeri, A. Cellulose acetate blends − effect of plasticizers on properties and biodegradability. *J. Renewable Mater.* **2014**, *2*, 35−41.

(6) Mohanty, A. K.; Wibowo, A.; Misra, M.; Drzal, L. T. Effect of process engineering on the performance of natural fiber reinforced cellulose acetate biocomposites. *Compos. A Appl. Sci. Manuf.* **2004**, *35*, 363−370.

(7) Misra, M.; Mohanty, A. K.; Drzal, L. T. Sustainable biocomposites from renewable resources: opportunities and challenges in the green materials world. *J. Polym. Environ.* **2002**, *10*, 19−26.

(8) Wojciechowska, P. *Recent Advances in Plasticizers*; Luqman, M., Ed.; InTech: Rijeka, Croatia, 2012; pp. 141−164.

(9) Kolb, H. C.; Finn, M. G.; Sharpless, K. B. Click chemistry: diverse chemical function from a few good reactions. *Angew. Chem., Int. Ed.* **2001**, *40*, 2004−2021.
(10) Meng, X.; Edgar, K. J. "Click" reactions in polysaccharide modification. *Prog. Polym. Sci.* **2016**, *53*, 52−85.
(11) Hoyle, C. E.; Bowman, C. N. Thiol-ene click chemistry. *Angew. Chem., Int. Ed.* **2010**, *49*, 1540−1573.
(12) Lowe, A. B. Thiol-ene "click" reactions and recent applications in polymer and materials synthesis: a first update. *Polym. Chem.* **2014**, *5*, 4820−4870.
(13) Nair, D. P.; Podgórski, M.; Chatani, S.; Gong, T.; Xi, W.; Fenoli, C. R.; Bowman, C. N. The thiol-Michael addition click reaction: a powerful and widely used tool in materials chemistry. *Chem. Mater.* **2014**, *26*, 724−744.
(14) Tingaut, P.; Hauert, R.; Zimmermann, T. Highly efficient and straightforward functionalization of cellulose films with thiol-ene click chemistry. *J. Mater. Chem.* **2011**, *21*, 16066−16076.
(15) Zhao, G.-L.; Hafrén, J.; Deiana, L.; Córdova, A. Heterogeneous "organoclick" derivatization of polysaccharides: photochemical thiol-ene click modification of solid cellulose. *Macromol. Rapid Commun.* **2010**, *31*, 740−744.
(16) Meng, X.; Choudhury, S. R.; Edgar, K. J. Multifunctional cellulose esters by olefin cross-metathesis and thiol-Michael addition. *Polym. Chem.* **2016**, *7*, 3848−3856.
(17) Moreira, G.; Fedeli, E.; Ziarelli, F.; Capitani, D.; Mannina, L.; Charles, L.; Viel, S.; Gigmes, D.; Lefay, C. Synthesis of polystyrene-grafted cellulose acetate copolymers via nitroxide-mediated polymerization. *Polym. Chem.* **2015**, *6*, 5244−5253.
(18) Breu, J.; Seidl, W.; Stoll, A. J.; Lange, K. G.; Probst, T. U. Charge homogeneity in synthetic fluorohectorite. *Chem. Mater.* **2001**, *13*, 4213−4220.
(19) Stöter, M.; Kunz, D. A.; Schmidt, M.; Hirsemann, D.; Kalo, H.; Putz, B.; Senker, J.; Breu, J. Nanoplatelets of sodium hectorite showing aspect ratios of ∼20000 and superior purity. *Langmuir* **2013**, *29*, 1280−1285.
(20) Huang, F.-Y.; Wu, X.-J.; Yu, Y.; Lu, Y.-H. Preparation and properties of cellulose laurate (CL)/starch nanocrystals acetate (SNA) bio-nanocomposites. *Polymers* **2015**, *7*, 1331−1345.
(21) Zhang, Q.; Wang, X.; Decker, V.; Meyerhoff, M. E. Plasticizer-free thin-film sodium-selective optodes inkjet-printed on transparent plastic for sweat analysis. *ACS Appl. Mater. Interface* **2020**, *12*, 25616−25624.
(22) Luoma, E.; Välimäki, M.; Ollila, J.; Heikkinen, K.; Immonen, K. Bio-based polymeric substrates for printed hybrid electronics. *Polymers* **2022**, *14*, 1863.
(23) Raouf, R. M.; Wahab, Z. A.; Ibrahim, N. A.; Talib, Z. A.; Chieng, B. W. Transparent blend of poly(methylmethacrylate)/cellulose acetate butyrate for the protection from ultraviolet. *Polymers* **2016**, *8*, 128.
(24) Tran, T. N.; Mai, B. T.; Setti, C.; Athanassiou, A. Transparent bioplastic derived from CO_2-based polymer functionalized with oregano waste extract toward active food packaging. *ACS Appl. Mater. Interfaces* **2020**, *12*, 46667−46677.
(25) Arrieta, M. P.; Garrido, L.; Faba, S.; Galotto, M. J.; de Dicastillo, C. L. *Cucumis metuliferus* fruit extract loaded acetate cellulose coatings for antioxidant active packaging. *Polymers* **2020**, *12*, 1248.
(26) Lange, J.; Wyser, Y. Recent innovations in barrier technologies for plastic packaging − a review. *Packaging Technol. Sci.* **2003**, *16*, 149−158.
(27) Thomas, S.; Joseph, K.; Malhotra, S. K.; Goda, K.; Sreekala, M. S. *Polymer Composites, Macro- and Microcomposites*; Wiley-VCH Verlag: Weinheim, Germany, 2012.
(28) Cussler, E. L.; Hughes, S. E.; Ward, W. J.; Aris, R. Barrier membranes. *J. Membr. Sci.* **1988**, *38*, 161−174.
(29) Habel, C.; Schöttle, M.; Daab, M.; Eichstaedt, N. J.; Wagner, D.; Bakhshi, H.; Agarwal, S.; Horn, M. A.; Breu, J. High-barrier, biodegradable food packaging. *Macromol. Mater. Eng.* **2018**, *303*, No. 1800333.
(30) Habel, C.; Tsurko, E. S.; Timmins, R. L.; Hutschreuther, J.; Kunz, R.; Schuchardt, D. D.; Rosenfeldt, S.; Altstädt, V.; Breu, J. J. Lightweight ultra-high-barrier liners for helium and hydrogen. *ACS Nano* **2020**, *14*, 7018−7024.
(31) Schilling, T.; Habel, C.; Rosenfeldt, S.; Röhrl, M.; Breu, J. Impact of ultraconfinement on composite barriers. *ACS Appl. Polym. Mater.* **2020**, *2*, 3010−3015.
(32) Röhrl, M.; Federer, L.; Timmins, R. L.; Rosenfeldt, S.; Dörres, T.; Habel, C.; Breu, J. Disorder−order transition—improving the moisture sensitivity of waterborne nanocomposite barriers. *ACS Appl. Mater. Interfaces* **2021**, *13*, 48101−48109.
(33) Dudko, V.; Ottermann, K.; Rosenfeldt, S.; Papastavrou, G.; Breu, J. Osmotic delamination: a forceless alternative for the production of nanosheets now in highly polar and aprotic solvents. *Langmuir* **2021**, *37*, 461−468.
(34) Timmins, R. L.; Kumar, A.; Röhrl, M.; Havlícek, K.; Agarwal, S.; Breu, J. High barrier nanocomposite film with accelerated biodegradation by clay swelling induced fragmentation. *Macromol. Mater. Eng.* **2022**, *307*, No. 2100727.

https://doi.org/10.1021/acsomega.2c06811
ACS Omega 2023, 8, 9889−9895